SCIENCE AND TECHNOLOGY ORGANIZATION
CENTRE FOR MARITIME RESEARCH AND EXPERIMENTATION

Reprint Series **CMRE-PR-2019-069**

Localization of multiple sources using time-difference of arrival measurements

Florian Meyer, Alessandra Tesei, Moe Z. Win

June 2019

Originally published in:

2017 IEEE International Conference on Acoustics, Speech and Signal Processing (ICASSP), 5-9 March 2017, New Orleans, USA, pp.3151-3155, doi: 10.1109/ICASSP.2017.7952737

About CMRE

The Centre for Maritime Research and Experimentation (CMRE) is a world-class NATO scientific research and experimentation facility located in La Spezia, Italy.

The CMRE was established by the North Atlantic Council on 1 July 2012 as part of the NATO Science & Technology Organization. The CMRE and its predecessors have served NATO for over 50 years as the SACLANT Anti-Submarine Warfare Centre, SACLANT Undersea Research Centre, NATO Undersea Research Centre (NURC) and now as part of the Science & Technology Organization.

CMRE conducts state-of-the-art scientific research and experimentation ranging from concept development to prototype demonstration in an operational environment and has produced leaders in ocean science, modelling and simulation, acoustics and other disciplines, as well as producing critical results and understanding that have been built into the operational concepts of NATO and the nations.

CMRE conducts hands-on scientific and engineering research for the direct benefit of its NATO Customers. It operates two research vessels that enable science and technology solutions to be explored and exploited at sea. The largest of these vessels, the NRV Alliance, is a global class vessel that is acoustically extremely quiet.

CMRE is a leading example of enabling nations to work more effectively and efficiently together by prioritizing national needs, focusing on research and technology challenges, both in and out of the maritime environment, through the collective Power of its world-class scientists, engineers, and specialized laboratories in collaboration with the many partners in and out of the scientific domain.

NOTE: The CMRE Reprint series reprints papers and articles published by CMRE authors in the open literature as an effort to widely disseminate CMRE products. Users are encouraged to cite the original article where possible.

LOCALIZATION OF MULTIPLE SOURCES USING TIME-DIFFERENCE OF ARRIVAL MEASUREMENTS

Florian Meyer⋆ Alessandra Tesei⋆, and Moe Z. Win†

⋆Centre for Maritime Research and Experimentation, La Spezia, Italy

†Laboratory for Information and Decision Systems, Massachusetts Institute of Technology, Cambridge, MA, USA

ABSTRACT

This paper addresses the problem of localizing an unknown number of static sources emitting unknown signals from time-difference of arrival (TDOA) measurements. Based on the framework of random finite sets and finite set statistics, we formulate the Bayesian estimation problem and develop a particle-based localization algorithm that overcomes the challenges related to the highly non-linear TDOA measurement model, the data associations uncertainty, and the uncertainty in the number of sources to be localized. Simulation results confirm that the number of sources can be determined correctly and accurate location estimates can be obtained when the number of false alarms is low and the probability of detection is high.

***Index Terms*—** Time-difference of arrival, random finite sets, multiobject estimation, finite set statistics, sequential Monte Carlo techniques.

1. INTRODUCTION

We address the problem of localizing multiple sources from their electromagnetic or acoustic signals, when the absolute time of transmission is unknown. The proposed approach uses time-difference of arrival (TDOA) location information [1] related to peaks in the cross-correlation function of multiple spatially separated receivers. TDOA-based localization has wide applications in wireless communication [2–5] and passive surveillance systems [6–9] and is potentially more accurate compared to traditional triangulation approaches that use angular measurements.

1.1. TDOA Location Information and Random Finite Sets

Fig. 1 shows the hyperbolic TDOA location information for three non-cooperative sources provided by a synchronized cooperative receiver pair. Hyperbolic TDOA location information related to different receiver pairs is expected to intersect in the vicinity of true source locations. Localization of multiple sources is complicated by data association uncertainty, i.e., it is not known which TDOA measurement is associated to a specific source. In addition, due to fading in the propagation path, the signal of certain sources might be missing at some receivers or false TDOA measurements which are not related to a source might be erroneously extracted. These two effects are typically referred to as missed detection and false alarms, respectively. Thus, the number of extracted TDOA measurements might be different among receiver pairs. Furthermore, the number of sources to be localized is unknown. Traditional methods for TDOA-based localization (see [1, 9, 10] and references therein) typically assume a single source and do not consider missed detections and false alarms.

This work was supported by the NATO Supreme Allied Command Transformation under project SAC000601 and by the FWF under grant J3886-N31. F. Meyer is currently with Laboratory for Information and Decision Systems, Massachusetts Institute of Technology, Cambridge, MA, USA.

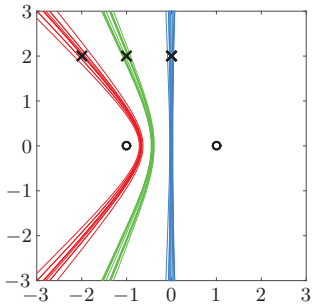

Fig. 1. The hyperbolic functions related to TDOA measurements of two receivers (indicated by circles) for three sources (indicated by crosses) for different noise realizations.

For the estimation of an unknown number of objects in the presence of data association uncertainty, random finite sets (RFSs) and finite set statistics (FISST) offer attractive solutions [11]. Techniques for tracking an unknown number of objects based on the FISST framework include the probability hypothesis density (PHD) filter [11–13], the cardinalized PHD filter [11, 14, 15], (labeled) multi-Bernoulli filters [11, 16, 17], and the recently proposed track-oriented marginal multi-Bernoulli/Poisson (TOMB/P) filter [18, 19]. The TOMB/P uses a hybrid Bernoulli/Poisson RFS model and provides an accurate approximation of the full Bayesian RFS filter.

1.2. Contribution and Paper Organization

In this paper, we state the Bayesian estimation problem for the TDOA-based localization of an unknown number of static sources. Based on the hybrid Bernoulli/Poisson model introduced in the TOMB/P filter [18, 19], we develop a particle-based localization algorithm that overcomes the challenges related to the highly non-linear TDOA measurement model, the data associations uncertainty, and the uncertainty in the number of sources to be localized. Simulation results confirm that the number of sources can be determined correctly and accurate location estimates can be obtained when the number of false alarms is low and the probability of detection is high.

This paper is organized as follows. The basics of RFSs are reviewed in Section 2. The system model is described in Section 3. In Section 4 the RFS based estimation problem is formulated and the proposed method is presented. Simulation results are reported in Section 5.

2. RFS BASICS

A random quantity X whose realizations $\mathcal{X} = \{\mathbf{x}^{(1)}, \ldots, \mathbf{x}^{(n)}\}$ are finite sets of n_x-dimensional vectors $\mathbf{x}^{(1)}, \ldots, \mathbf{x}^{(n)} \in \mathbb{R}^{n_x}$ is referred to as a RFS. Both the number $n = |\mathcal{X}|$, $n \in \mathbb{N}_0$ of vectors in the set (the cardinality of $\mathcal{X}$) and the vectors $\mathbf{x}^{(i)}$ are chosen randomly. Thus, X consists of a random number $\mathsf{n} = |\mathsf{X}|$ of random vectors $\mathbf{x}^{(1)}, \ldots, \mathbf{x}^{(\mathsf{n})}$. For the case of zero cardinality ($n = 0$), we have $\mathcal{X} = \emptyset$. Note that the elements $\mathbf{x}^{(1)}, \ldots, \mathbf{x}^{(n)}$ of a set $\mathcal{X} = \{\mathbf{x}^{(1)}, \ldots, \mathbf{x}^{(n)}\}$ are unordered.

Adopting the FISST framework [11], the statistics of a RFS X can be described by the multiobject probability density function (pdf) $f_{\mathsf{X}}(\mathcal{X})$ that is briefly denoted $f(\mathcal{X})$. For any realization $\mathcal{X} = \{\mathbf{x}^{(1)}, \ldots, \mathbf{x}^{(n)}\}$, $f(\mathcal{X})$ can be evaluated as

$$f(\mathcal{X}) = n!\, \rho(n)\, f_n(\mathbf{x}^{(1)}, \ldots, \mathbf{x}^{(n)}), \tag{1}$$

where, $\rho(n) \triangleq \Pr\{|\mathsf{X}| = n\}$ is the probability mass function of the random cardinality n—termed the cardinality distribution—and $f_n(\mathbf{x}^{(1)}, \ldots, \mathbf{x}^{(n)})$ is a pdf of n random vectors $\mathbf{x}^{(1)}, \ldots, \mathbf{x}^{(n)}$ that is symmetric, i.e., invariant to argument permutation. For the case of zero cardinality, $f(\emptyset) = \rho(0)$.

Next, we review three types of RFSs that are relevant for the proposed estimation scheme. The *Poisson RFS* X has a cardinality that follows a Poisson distribution with mean μ, i.e., $\rho(n) = e^{-\mu}\mu^n/n!$, $n \in \mathbb{N}_0$. (Note that a Poisson distribution is fully characterized by its means which is at the same time its variance.) For any n, the elements of a Poisson RFS $\mathbf{x}^{(1)}, \ldots, \mathbf{x}^{(n)}$ of X are independent and identically distributed (iid) according to its "spatial pdf" $f(\mathbf{x})$, i.e., $f_n(\mathbf{x}^{(1)}, \ldots, \mathbf{x}^{(n)}) = \prod_{i=1}^{n} f(\mathbf{x}^{(i)})$. From (1), the multiobject pdf can thus be obtained as

$$f(\mathcal{X}) = e^{-\mu} \prod_{\mathbf{x} \in \mathcal{X}} \mu f(\mathbf{x}).$$

The product $\mu f(\mathbf{x})$ is referred to as intensity function or PHD and fully characterizes a Poisson RFS.

A *Bernoulli RFS* X with probability of existence r and spatial pdf $f(\mathbf{x})$ is empty with probability $1 - r$ and contains one element $\mathbf{x} \sim f(\mathbf{x})$ with probability r. Hence, the multiobject pdf is

$$f(\mathcal{X}) = \begin{cases} 1-r, & \mathcal{X} = \emptyset, \\ r\, f(\mathbf{x}), & \mathcal{X} = \{\mathbf{x}\}, \\ 0, & \text{otherwise.} \end{cases}$$

A *multi-Bernoulli RFS* X is the union of independent Bernoulli RFSs $\mathsf{X}^{(j)}$, $j \in \{1, \ldots, J\}$ with existence probabilities $r^{(j)}$ and spatial pdfs $f^{(j)}(\mathbf{x})$, i.e., $\mathsf{X} = \bigcup_{j=1}^{J} \mathsf{X}^{(j)}$. Every Bernoulli RFSs $\mathsf{X}^{(j)}$, $j \in \{1, \ldots, J\}$ is referred to as a component of X. The multiobject pdf $f(\mathcal{X})$ of the multi-Bernoulli RFS X is parametrized by $r^{(j)}$ and $f^{(j)}(\mathbf{x})$, $j \in \{1, \ldots, J\}$ and can be obtained using FISST convolution. For an union of two RFS, i.e., $\mathsf{X} = \mathsf{X}_1 \cup \mathsf{X}_2$ calculating the multiobject pdf $f(\mathcal{X})$ by means of FISST convolution is defined as [11, 18]

$$f_{\mathsf{X}}(\mathcal{X}) = \sum_{\mathcal{Y} \subseteq \mathcal{X}} f_{\mathsf{X}_1}(\mathcal{Y})\, f_{\mathsf{X}_2}(\mathcal{X} \backslash \mathcal{Y}). \tag{2}$$

3. SYSTEM MODEL

Consider the localization of multiple passive sources using n_{r} receivers in 2D in known locations $\mathbf{q}^{(k)} = [q_x^{(k)}\, q_y^{(k)}]^{\mathrm{T}}$. The number of sources n_{t} and their unknown locations $\mathbf{p}^{(j)} = [\mathsf{p}_x^{(j)}\, \mathsf{p}_y^{(j)}]^{\mathrm{T}}$ are random and can be denoted consistently using a RFS P. Receivers can exchange their received signals and are perfectly synchronized.

3.1. TDOA Measurements

A simple way to obtain location information of non-synchronized sources with unknown waveforms, is to compare signals at the receivers pairwise. More specifically, for each receiver pair (k, l) the signal of receiver k and the signal of receiver l are correlated and time delays $r_{kl}^{(m)}$, $m = 1, \ldots, n_{kl}$ related to peaks in the resulting cross-correlation function are extracted. These time delays are referred to as a TDOA measurements [1].

Each TDOA measurement $r_{kl}^{(m)}$ is related to a possible source location $\mathbf{p}^{(j)}$ along a hyperbola. For receiver pair (k, l), the random TDOA $\mathsf{r}_{kl}^{(m)}$ that was originated by source j is modeled as

$$\begin{aligned} \mathsf{r}_{kl}^{(m)} &= \frac{1}{v}\Big(\|\mathbf{p}^{(j)} - \mathbf{q}^{(k)}\| - \|\mathbf{p}^{(j)} - \mathbf{q}^{(l)}\|\Big) + \mathsf{z}_{kl}^{(m)} \\ &= h_{kl}(\mathbf{p}^{(j)}) + \mathsf{z}_{kl}^{(m)}, \end{aligned} \tag{3}$$

where v is the propagation speed and $\mathsf{z}_{kl}^{(m)}$ is the measurement noise which is zero-mean Gaussian with variance σ_z^2 and statistically independent across m and (k, l) pairs. The dependence of a measured TDOA $r_{kl}^{(m)}$ on the location $\mathbf{p}^{(j)}$ of the generating source j is described by the likelihood function $f(r_{kl}^{(m)}|\mathbf{p}^{(j)})$ that can be directly obtained from (3). For receivers k, l located at $\mathbf{q}^{(k)} = [q_x, 0]^{\mathrm{T}}$ and $\mathbf{q}^{(l)} = [-q_x, 0]^{\mathrm{T}}$, (3) reads

$$\mathsf{r}_{kl}^{(m)} = \frac{1}{v}\left[\sqrt{\left(\mathsf{p}_x^{(j)} - q_x\right)^2 + \mathsf{p}_y^{(j)\,2}} - \sqrt{\left(\mathsf{p}_x^{(j)} + q_x\right)^2 + \mathsf{p}_y^{(j)\,2}}\right] + \mathsf{z}_{kl}^{(m)}. \tag{4}$$

Let $r_{kl}^{(m)}$ be a measured TDOA according to (4) and let us neglect its unknown noise realization, i.e., $z_{kl}^{(m)} = 0$. After some algebra, (4) can be written in the form of a hyperbola as

$$\frac{p_x^{(j)\,2}}{a^2} - \frac{p_y^{(j)\,2}}{b^2} = \frac{p_x^{(j)\,2}}{(r_{kl}^{(m)}\, v)^2/4} - \frac{p_y^{(j)\,2}}{q_x^2 - (r_{kl}^{(m)}\, v)^2/4} = 1.$$

Fig. 1 shows the related hyperbolas for three sources with locations $[0\ 2]^{\mathrm{T}}$, $[-1\ 2]^{\mathrm{T}}$, and $[-2\ 2]^{\mathrm{T}}$, and different realizations of $\mathsf{z}_{kl}^{(m)}$.

3.2. Multiobject Likelihood Function and Prior Distribution

The n_{kl} TDOA measurements related to receiver pair (k, l) are modeled as a RFS R_{kl}. The probability that the source j gives rise to a measurement $r_{kl}^{(m)}$ is p_{d}. Therefore, the measurement related to source j is modeled as a Bernoulli RFS $\Theta_{kl}\big(\mathbf{p}^{(j)}\big)$ with existence probability $r = p_{\mathrm{d}}$ and spatial pdf $f\big(r_{kl}^{(m)}\big) = f\big(r_{kl}^{(m)}|\mathbf{p}^{(j)}\big)$. This leads to the following RFS likelihood function related to source j,

$$f\big(\mathcal{R}_{kl}|\mathbf{p}^{(j)}\big) = \begin{cases} 1 - p_{\mathrm{d}}, & \mathcal{R}_{kl} = \emptyset, \\ p_{\mathrm{d}}\, f\big(r_{kl}^{(m)}|\mathbf{p}^{(j)}\big), & \mathcal{R}_{kl} = \big\{r_{kl}^{(m)}\big\}, \\ 0, & \text{otherwise.} \end{cases}$$

We adopt the standard assumption, that a measurement $r_{kl}^{(m)}$ cannot originate from more than one source simultaneously, and one source can generate at most one measurement $r_{kl}^{(m)}$ at each receiver pair [11, 20]. Thus, all source-originated measurements form the multi-Bernoulli RFS $\bigcup_{j=1}^{n_{\mathrm{t}}} \Theta_{kl}\big(\mathbf{p}^{(j)}\big)$.

Following [11, 20], it is assumed that the number of false alarms at receiver pair (k, l) is Poisson distributed with mean μ. Furthermore, at each receiver pair (k, l), the false alarms denoted by K_{kl}

are assumed to be independent of the source-originated measurements and independent and identically distributed (iid) according to the spatial pdf $f_{\mathrm{c}}(r_{kl}^{(m)})$. Assuming that each measurement $r_{kl}^{(m)}$ originates either from a source or is a false alarm, the overall measurement RFS at receiver pair (k,l), R_{kl}, is then obtained as

$$\mathsf{R}_{kl} = \bigcup_{j=1}^{n_{\mathrm{t}}} \Theta_{kl}(\mathbf{p}^{(j)}) \cup \mathsf{K}_{kl}. \tag{5}$$

The dependence of the overall measurement RFS R_{kl} on the overall source location RFS P, is described by the multiobject likelihood function $f(\mathcal{R}_{kl}|\mathcal{P})$, which can be obtain from (5) using FISST convolution (cf. (2)). Let every receiver pair be one of $n_{\mathrm{s}} = \binom{n_{\mathrm{r}}}{2}$ sensors s with corresponding receiver indexes (k_s, l_s) and let $\mathcal{R}_{1:n_{\mathrm{s}}} \triangleq \big(\mathcal{R}_{k_1 l_1}, \ldots, \mathcal{R}_{k_{n_{\mathrm{s}}} l_{n_{\mathrm{s}}}}\big)$ be an ordered list of single sensor measurements. The all-sensor likelihood function then reads

$$f(\mathcal{R}_{1:n_{\mathrm{s}}}|\mathcal{P}) = \prod_{s=1}^{n_{\mathrm{s}}} f(\mathcal{R}_{k_s l_s}|\mathcal{P}).$$

The prior pdf of P, $f(\mathcal{P})$, is modeled as a *Poisson RFS* with mean parameter μ_{p} and a spatial pdf $f_{\mathrm{p}}(\mathbf{p})$ that is chosen uniform on the 2D region of interest.

4. MULTIOBJECT ESTIMATION

In a Bayesian RFS setting, multiobject estimation relies on the marginal posterior pdf $f(\mathcal{P}|\mathcal{R}_{1:n_{\mathrm{s}}})$ after making the measurements $\mathcal{R}_{1:n_{\mathrm{s}}} \triangleq (\mathcal{R}_{k_1 l_1}, \ldots, \mathcal{R}_{k_{n_{\mathrm{s}}} l_{n_{\mathrm{s}}}})$. In our approach, this pdf is calculated by performing an update step for each sensor recursively, i.e., a single sensor update step is performed n_{s} times. At recursion s, $f(\mathcal{P}|\mathcal{R}_{1:s-1})$ is transformed into $f(\mathcal{P}|\mathcal{R}_{1:s})$. (Note that $f(\mathcal{P}|\mathcal{R}_{1:1}) \triangleq f(\mathcal{P}|\mathcal{R}_1)$ and $f(\mathcal{P}|\mathcal{R}_{1:0}) \triangleq f(\mathcal{P})$). We denote by P_s the RFS related to the pdf $f(\mathcal{P}|\mathcal{R}_{1:s})$.

Following [18] all updated multiobject state RFS P_s are modeled as the union of independent RFSs $\mathsf{P}_s^{\mathrm{u}}$ and $\mathsf{P}_s^{\mathrm{d}}$, i.e., $\mathsf{P}_s = \mathsf{P}_s^{\mathrm{u}} \cup \mathsf{P}_s^{\mathrm{d}}$, describing the undetected and detected sources, respectively. Let $f_s^{\mathrm{u}}(\mathcal{P})$ be the pdf of $\mathsf{P}_s^{\mathrm{u}}$ (note that $\mathsf{P}_s^{\mathrm{u}}$ is independent of $\mathcal{R}_{1:s}$ but not of s) and $f^{\mathrm{d}}(\mathcal{P}|\mathcal{R}_{1:s})$ be the posterior pdf related to $\mathsf{P}_s^{\mathrm{d}}$. Thus, the posterior multiobject pdf $f(\mathcal{P}|\mathcal{R}_{1:s})$ is given by the FISST convolution (cf. (2)). Note that $\mathsf{P}_s^{\mathrm{u}}$ is a Poisson RFS with mean parameter μ_s^{u}, spatial pdf $f_s^{\mathrm{u}}(\mathbf{p})$, and intensity function $\lambda_s^{\mathrm{u}}(\mathbf{p}) = \mu_s^{\mathrm{u}} f_s^{\mathrm{u}}(\mathbf{p})$. Furthermore, $\mathsf{P}_s^{\mathrm{d}}$ is a multi-Bernoulli RFS consisting of J_s Bernoulli components with existence probabilities $r_s^{(j)}$ and spatial pdfs $f_s^{(j)}(\mathbf{p}), j \in \{1, \ldots, J_s\}$, where each Bernoulli component represents a potential source and its location. For $s = 0$, we have $\lambda_0^{\mathrm{u}} = \mu_{\mathrm{p}} f_{\mathrm{p}}(\mathbf{p})$ and $J_0 = 0$.

4.1. Single Sensor Update

The intensity function $\lambda_s^{\mathrm{u}}(\mathbf{p})$ related to the Poisson pdf $f_s^{\mathrm{u}}(\mathcal{P})$ at recursion s, can be calculated directly from $\lambda_{s-1}^{\mathrm{u}}(\mathbf{p})$ as

$$\lambda_s^{\mathrm{u}}(\mathbf{p}) = (1 - p_{\mathrm{D}})\, \lambda_{s-1}^{\mathrm{u}}(\mathbf{p}).$$

However, the update step for the detected sources yields a *weighted mixture* of multi-Bernoulli pdfs with a number of components that grow exponentially in the number of sensors n_{s}. To obtain an approximation $\tilde{f}^{\mathrm{d}}(\mathcal{P}|\mathcal{R}_{1:s})$ for $f^{\mathrm{d}}(\mathcal{P}|\mathcal{R}_{1:s})$ that is still a multi-Bernoulli RFS and to avoid an exponential scaling of the computational complexity in the number of sensors n_{s}, an approximation presented in the context of multiobject tracking [18] was adopted.

The approximated multi-Bernoulli pdf $\tilde{f}^{\mathrm{d}}(\mathcal{P}|\mathcal{R}_{1:s})$ is characterized by existence probabilities $r_s^{(j)}$ and spatial pdfs $f_s^{(j)}(\mathbf{p})$ related to the Bernoulli components $f_s^{(j)}(\mathcal{P})$, $j \in \{1, \ldots, J_s\}$. Therefore, the update step amounts to calculating these quantities from $\lambda_{s-1}^{\mathrm{u}}(\mathbf{p})$, $r_{s-1}^{(j)}$ and $f_{s-1}^{(j)}(\mathbf{p})$, $j \in \{1, \ldots, J_{s-1}\}$. Note that the number of Bernoulli components in $\tilde{f}^{\mathrm{d}}(\mathcal{P}|\mathcal{R}_{1:s})$ is $J_s = J_{s-1} + n_{k_s l_s}$, consisting of one "legacy" Bernoulli component $j \in \{1, \ldots, J_{s-1}\}$ for each component in $\tilde{f}^{\mathrm{d}}(\mathcal{P}|\mathcal{R}_{1:s-1})$ and one new component $j \in \{J_{s-1}+1, \ldots, J_{s-1}+n_{k_s l_s}\}$ for each of the $n_{k_s l_s}$ measurements $r_{kl}^{(m)}$, $m \in \{1, \ldots, n_{k_s l_s}\}$. The calculations of updated Bernoulli components is based on so-called marginal association probabilities $p_s^{(j)}(m)$, $j \in \{1, \ldots, J_s\}$ [20]. For efficient calculation of marginal association probabilities by means of loopy belief propagation we refer the reader to [21].

The legacy components $j \in \{1, \ldots, J_{s-1}\}$, can be obtained as

$$r_s^{(j)} = p_s^{(j)}(0)\, \frac{r_{s-1}^{(j)}(1-p_{\mathrm{D}})}{1 - r_{s-1}^{(j)} p_{\mathrm{D}}} + \sum_{m=1}^{n_{k_s l_s}} p_s^{(j)}(m),$$

$$f_s^{(j)}(\mathbf{p}) = \frac{f_{s-1}^{(j)}(\mathbf{p})}{r_s^{(j)}} \Bigg[p_s^{(j)}(0)\, \frac{r_{s-1}^{(j)}(1-p_{\mathrm{D}})}{1 - r_{s-1}^{(j)} p_{\mathrm{D}}} + \sum_{m=1}^{n_{k_s l_s}} p_s^{(j)}(m)\, \frac{f\big(r_{kl}^{(m)}|\mathbf{p}\big)}{\int f\big(r_{kl}^{(m)}|\mathbf{p}\big) f_{s-1}^{(j)}(\mathbf{p}) \mathrm{d}\mathbf{p}} \Bigg]. \tag{6}$$

Furthermore, the new components $j = J_{s-1} + m$ with $m \in \{1, \ldots, n_{k_s l_s}\}$, are given by

$$r_s^{(j)} = \frac{p_s^{(j)}(m)\, p_{\mathrm{D}} \int f\big(r_{kl}^{(m)}|\mathbf{p}\big)\, \lambda_{s-1}^{\mathrm{u}}(\mathbf{p})\, \mathrm{d}\mathbf{p}}{\lambda_{\mathrm{c}}\big(r_{kl}^{(m)}\big) + p_{\mathrm{D}} \int f\big(r_{kl}^{(m)}|\mathbf{p}\big)\, \lambda_{s-1}^{\mathrm{u}}(\mathbf{p})\, \mathrm{d}\mathbf{p}}, \tag{7}$$

$$f_s^{(j)}(\mathbf{p}) = \frac{f\big(r_{kl}^{(m)}|\mathbf{p}\big)\, \lambda_{s-1}^{\mathrm{u}}(\mathbf{p})}{\int f\big(r_{kl}^{(m)}|\mathbf{p}\big)\, \lambda_{s-1}^{\mathrm{u}}(\mathbf{p}) \mathrm{d}\mathbf{p}}. \tag{8}$$

The expression in (6), (7), and (8) can not be evaluated in closed form. Thus, we employ a sequential Monte Carlo implementation for approximate evaluation of (6), (7), and (8). First, the integrals $\int f\big(r_{kl}^{(m)}|\mathbf{p}\big) f_{s-1}^{(j)}(\mathbf{p}) \mathrm{d}\mathbf{p}$ and $\int f\big(r_{kl}^{(m)}|\mathbf{p}\big)\, \lambda_{s-1}^{\mathrm{u}}(\mathbf{p})\, \mathrm{d}\mathbf{p}$ are evaluated using Monte Carlo integration [22]. Next, for each $j \in \{1, \ldots, J_s\}$, L particles and corresponding weights $\big\{\big(\mathbf{p}_s^{(j,l)}, w_s^{(j,l)}\big)\big\}_{l=1}^{L}$ representing $f_s^{(j)}(\mathbf{p})$ are calculated by means of importance sampling [22] using as proposal pdf $f_{s-1}^{(j)}(\mathbf{p})$ in (6) and $f_{s-1}^{\mathrm{u}}(\mathbf{p})$ in (8), respectively. A particle-based calculation of the marginal association probabilities $p_s^{(j)}(m)$, $j \in \{1, \ldots, J_s\}$ is presented in [19].

4.2. Detection and Estimation

The Bernoulli component j in $\tilde{f}^{\mathrm{d}}(\mathcal{P}|\mathcal{R}_{1:n_{\mathrm{s}}})$ is considered to exist if $r_{n_{\mathrm{s}}}^{(j)} > 0.5$. For each component j that is considered to exist, an estimate of the source location $\mathbf{p}^{(j)}$ can then be calculated as

$$\hat{\mathbf{p}}^{(j)} \triangleq \sum_{l=1}^{L} \mathbf{p}_{n_{\mathrm{s}}}^{(j,l)} w_{n_{\mathrm{s}}}^{(j,l)}.$$

The entirety of all $\hat{n}_{\mathrm{t}}$ detected location estimates $\hat{\mathbf{p}}^{(j)}$ forms the estimated set $\hat{\mathcal{P}} = \{\hat{\mathbf{p}}^{(1)}, \ldots, \hat{\mathbf{p}}^{\hat{n}_{\mathrm{t}}}\}$.

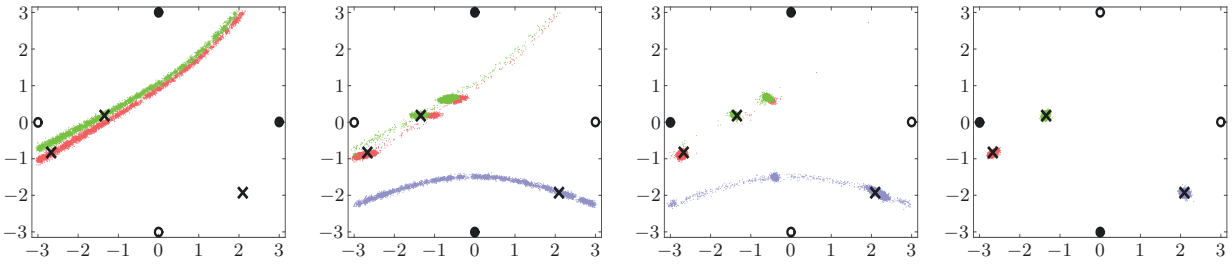

(a) (b) (c) (d)

Fig. 2. Particle-based representation of the spatial pdfs related to the three Bernoulli components with the highest existence probabilities in $f^d(\mathcal{P}|\mathcal{R}_{1:s})$: (a) $s = 1$, (b) $s = 2$, (c) $s = 3$, and (d) $s = 6 = n_s$. The locations of receivers involved in the current update step are indicated by dots, the locations of other receivers are indicated by circles.

5. SIMULATION RESULTS

In our simulations the sources are randomly placed on a region of interest of $[-3, 3] \times [-3, 3]$. The source-originated TDOAs $\mathsf{r}_{kl}^{(m)}$ at receiver pair (k, l) are distributed according to (3) with a standard deviation of $\sigma_z = 0.02/v$ for the noise $z_{kl}^{(m)}$. The false alarm pdf $f_{\text{FA}}(r_{kl}^{(m)})$ at receiver pair (k, l) is uniform on $\|\mathbf{q}^{(k)} - \mathbf{q}^{(l)}\|/v$. The receivers are located evenly on a circle of radius 3. The mean parameter of the prior pdf $f_{\text{p}}(\mathcal{P})$ was chosen as $\mu_{\text{p}} = 5$. The number of particles was set to $L = 50 \cdot 10^3$.

For a single realization, Fig. 2 shows simulation results for a scenario with $n_{\text{r}} = 4$ ($n_{\text{s}} = 6$), $p_{\text{D}} = 0.9$, and $\mu = 1$. More specifically, Fig. 2 shows particles representing the spatial pdfs of the three Bernoulli components with the highest existence probabilities of $\tilde{f}^{\text{d}}(\mathcal{P}|\mathcal{R}_1)$ in Fig. 2(a), of $\tilde{f}^{\text{d}}(\mathcal{P}|\mathcal{R}_{1:2})$ in Fig. 2(b), of $\tilde{f}^{\text{d}}(\mathcal{P}|\mathcal{R}_{1:3})$ in Fig. 2(c), and of $\tilde{f}^{\text{d}}(\mathcal{P}|\mathcal{R}_{1:6})$ in Fig. 2(d), respectively. A few remarks are in order:

- The first receiver pair ($s = 1$) has one missed detection and no false alarm measurement ($n_{k_1 l_1} = 2$); $\tilde{f}^{\text{d}}(\mathcal{P}|\mathcal{R}_1)$ consists only $J_1 = 2$ components. The spatial pdfs $f_1^{(1)}(\mathbf{p})$ and $f_1^{(2)}(\mathbf{p})$ meet the true locations of two sources.
- The second receiver pair ($s = 2$) has no missed detection and one false alarm measurement ($n_{k_2 l_2} = 4$); $\tilde{f}^{\text{d}}(\mathcal{P}|\mathcal{R}_{1:2})$ consists of $J_2 = J_1 + n_{k_2 l_2} = 6$ components. The two Bernoulli components with the highest existence probabilities are the legacy components that were generate from the measurements of the first receiver pair. Their spatial pdfs $f_2^{(1)}(\mathbf{p})$ and $f_2^{(2)}(\mathbf{p})$ have modes which correspond to the intersection points of the hyperbolas related to previous measurements and current measurements. The Bernoulli component $f_2^{(3)}(\mathbf{p})$ with the third-highest existence probability is related to a new measurement that does not intersect with an existent Bernoulli component.
- The third receiver pair ($s = 3$) has no missed detection and no false alarm measurement ($n_{k_3 l_3} = 3$); $\tilde{f}^{\text{d}}(\mathcal{P}|\mathcal{R}_{1:3})$ consists of $J_3 = J_2 + n_{k_3 l_3} = 9$ components. The spatial pdfs $f_3^{(1)}(\mathbf{p})$, $f_3^{(2)}(\mathbf{p})$, and $f_3^{(3)}(\mathbf{p})$ are still multimodal but more concentrated around the true source locations compared to the $s = 2$ result.
- After the update step has been performed for all $n_{\text{s}} = 6$ receiver pairs, $\tilde{f}^{\text{d}}(\mathcal{P}|\mathcal{R}_{1:n_{\text{s}}})$ consists of $J_{n_{\text{s}}} = 20$ components and the spatial pdfs related to the three components with the highest existence probabilities have a single mode that is well localized around the true locations of the three sources.

(p_d, μ)	$n_{\text{r}} = 4$		$n_{\text{r}} = 5$	
	$\bar{e}_{\text{L}}$	p_{C}	$\bar{e}_{\text{L}}$	p_{C}
$(.99, 0)$	$1.82 \cdot 10^{-2}$	0.01	$1.83 \cdot 10^{-2}$	0.00
$(.90, 0)$	$2.12 \cdot 10^{-2}$	0.01	$1.90 \cdot 10^{-2}$	0.00
$(.80, 0)$	$2.40 \cdot 10^{-2}$	0.01	$1.95 \cdot 10^{-2}$	0.00
$(.99, 1)$	$1.81 \cdot 10^{-2}$	0.01	$1.83 \cdot 10^{-2}$	0.00
$(.90, 1)$	$2.48 \cdot 10^{-2}$	0.09	$1.87 \cdot 10^{-2}$	0.01
$(.80, 1)$	$4.11 \cdot 10^{-2}$	0.29	$2.17 \cdot 10^{-2}$	0.06
$(.99, 2)$	$1.88 \cdot 10^{-2}$	0.02	$1.83 \cdot 10^{-2}$	0.01
$(.90, 2)$	$4.09 \cdot 10^{-2}$	0.23	$1.93 \cdot 10^{-2}$	0.02
$(.80, 2)$	$5.55 \cdot 10^{-2}$	0.46	$2.38 \cdot 10^{-2}$	0.10

Table 1. Simulated mean localization error $\bar{e}_{\text{L}}$ and probability of cardinality error p_{C} for different system parameters.

To investigate how the performance of our method depends on system parameters, we simulated scenarios with three different $p_{\text{D}} \in \{0.99, 0.9, 0.8\}$, three different $\mu \in \{0, 1, 2\}$ at each receiver pair, and two different $n_{\text{r}} \in \{4, 5\}$. The performance of the proposed method in terms of the probability of a cardinality error p_{C} and the mean localization error $\bar{e}_{\text{L}}$ is evaluated by simulations. For each realization, the localization error e_{L} is evaluated in terms of the OSPA metric [23] with a cut-off parameter of ∞ and with the Euclidean distance used as "inner metric." e_{L} only contributes to the mean localization error if the cardinality was estimated correctly.

Table 1 shows p_{C} and $\bar{e}_{\text{L}}$ for different values of n_{r}, p_{D}, and μ. For each possible combination of μ, p_{D}, and n_{r}, we performed 500 simulation runs. It can be seen that for low values of μ and high values of p_{D} all sources can be accurately localized. Furthermore, by comparing the results for $n_{\text{r}} = 4$ and $n_{\text{r}} = 5$ it is demonstrated how an increased number of receivers can improve both robustness of the cardinality estimate and localization accuracy in situations with an increased number of false alarms and a reduced probability of detection.

6. CONCLUSION

We presented a Bayesian algorithm for localizing an unknown number of static sources from TDOA measurements. The proposed algorithm is based on a recently introduced hybrid Bernoulli/Poisson filter and is implemented using sequential Monte Carlo techniques. Numerical results showed that for a low number of false alarms and a high probability of detection, all sources can be accurately localized. A possible direction for further research includes an improved approximation for the update step where data association is performed across multiple receiver pairs [24].

7. REFERENCES

[1] F. Gustafsson and F. Gunnarsson, "Positioning using time-difference of arrival measurements," in *Proc. IEEE ICASSP-03*, Hong Kong, China, Apr. 2003, vol. 6, pp. 553–556.

[2] C. Drane, M. Macnaughtan, and C. Scott, "Positioning GSM telephones," *IEEE Commun. Mag.*, vol. 36, no. 4, pp. 46–54, Apr. 1998.

[3] J. J. Caffery, *Wireless location in CDMA cellular radio systems*, Kluwer Academic, Norwell, MA, USA, 2000.

[4] A. Abrardo, G. Benelli, C. Maraffon, and A. Toccafondi, "Performance of TDoA-based radiolocation techniques in CDMA urban environments," in *Proc. IEEE ICC-02*, New York, NY, USA, Apr. 2002, vol. 1, pp. 431–435.

[5] R. Yamasaki, A. Ogino, T. Tamaki, T. Uta, N. Matsuzawa, and T. Kato, "TDOA location system for IEEE 802.11b WLAN," in *Proc. IEEE WCNC-05*, New Orleans, LA, USA, Mar. 2005, vol. 4, pp. 2338–2343.

[6] A. Quazi, "An overview on the time delay estimate in active and passive systems for target localization," *IEEE Trans. Acoust., Speech, and Signal Process.*, vol. 29, no. 3, pp. 527–533, Jun. 1981.

[7] Y. Huang, J. Benesty, G. W. Elko, and R. M. Mersereati, "Real-time passive source localization: A practical linear-correction least-squares approach," *IEEE Trans. Speech and Audio Process.*, vol. 9, no. 8, pp. 943–956, Nov. 2001.

[8] A. Dersan and Y. Tanik, "Passive radar localization by time difference of arrival," in *Proc. MILCOM-02*, Anaheim, CA, USA, Oct. 2002, vol. 2, pp. 1251–1257.

[9] D. Musicki, R. Kaune, and W. Koch, "Mobile emitter geolocation and tracking using TDOA and FDOA measurements," *IEEE Trans. Signal Process.*, vol. 58, no. 3, pp. 1863–1874, Mar. 2010.

[10] Y. Huang and J. Benesty, Eds., *Audio signal processing for next-generation multimedia communication systems*, Kluwer Academic, Boston, MA, USA, 2004.

[11] R. Mahler, *Statistical Multisource-Multitarget Information Fusion*, Artech House, Norwood, MA, USA, 2007.

[12] R. Mahler, "Multitarget Bayes filtering via first-order multitarget moments," *IEEE Trans. Aerosp. Electron. Syst.*, vol. 39, no. 4, pp. 1152–1178, Oct. 2003.

[13] B.-N. Vo, S. Singh, and A. Doucet, "Sequential Monte Carlo methods for multitarget filtering with random finite sets," *IEEE Trans. Aerosp. Electron. Syst.*, vol. 41, no. 4, pp. 1224–1245, Oct. 2005.

[14] R. Mahler, "PHD filters of higher order in target number," *IEEE Trans. Aerosp. Electron. Syst.*, vol. 43, no. 4, pp. 1523–1543, Oct. 2007.

[15] B.-T. Vo, B.-N. Vo, and A. Cantoni, "Analytic implementations of the cardinalized probability hypothesis density filter," *IEEE Trans. Signal Process.*, vol. 55, no. 7, pp. 3553–3567, Jul. 2007.

[16] B.-T. Vo, B.-N. Vo, and A. Cantoni, "The cardinality balanced multi-target multi-Bernoulli filter and its implementations," *IEEE Trans. Signal Process.*, vol. 57, no. 2, pp. 409–423, Feb. 2009.

[17] B.-T. Vo and B.-N. Vo, "Labeled random finite sets and multi-object conjugate priors," *IEEE Trans. Signal Process.*, vol. 61, no. 13, pp. 3460–3475, Jul. 2013.

[18] J. L. Williams, "Marginal multi-Bernoulli filters: RFS derivation of MHT, JIPDA and association-based MeMBer," *IEEE Trans. Aerosp. Electron. Syst.*, vol. 51, no. 3, pp. 1664–1687, Jul. 2015.

[19] T. Kropfreiter, F. Meyer, and F. Hlawatsch, "Sequential Monte Carlo implementation of the track-oriented marginal multi-Bernoulli/Poisson filter," in *Proc. FUSION-16*, Heidelberg, Germany, Jul. 2016, pp. 972–979.

[20] Y. Bar-Shalom and X.-R. Li, *Multitarget-Multisensor Tracking: Principles and Techniques*, Yaakov Bar-Shalom, Storrs, CT, USA, 1995.

[21] J. L. Williams and R. Lau, "Approximate evaluation of marginal association probabilities with belief propagation," *IEEE Trans. Aerosp. Electron. Syst.*, vol. 50, no. 4, pp. 2942–2959, Oct. 2014.

[22] A. Doucet, N. de Freitas, and N. Gordon, *Sequential Monte Carlo Methods in Practice*, Springer, New York, NY, 2001.

[23] D. Schuhmacher, B.-T. Vo, and B.-N. Vo, "A consistent metric for performance evaluation of multi-object filters," *IEEE Trans. Signal Process.*, vol. 56, no. 8, pp. 3447–3457, Aug. 2008.

[24] J. L. Williams and R. A. Lau, "Multiple scan data association by convex variational inference," *IEEE Trans. Signal Process.*, 2016, submitted, Available online: http://arxiv.org/abs/1607.07942.

Document Data Sheet

Security Classification		Project No.
Document Serial No.	**Date of Issue**	**Total Pages**
CMRE-PR-2019-069	June 2019	5 pp.

Author(s)

Florian Meyer, Alessandra Tesei, Moe Z. Win

Title

Localization of multiple sources using time-difference of arrival measurements

Abstract

This paper addresses the problem of localizing an unknown number of static sources emitting unknown signals from time-difference of arrival (TDOA) measurements. Based on the framework of random finite sets and finite set statistics, we formulate the Bayesian estimation problem and develop a particle-based localization algorithm that overcomes the challenges related to the highly non-linear TDOA measurement model, the data associations uncertainty, and the uncertainty in the number of sources to be localized. Simulation results confirm that the number of sources can be determined correctly and accurate location estimates can be obtained when the number of false alarms is low and the probability of detection is high.

Keywords

Time-difference of arrival, random finite sets, multiobject estimation, finite set statistics, sequential Monte Carlo techniques

Issuing Organization

NATO Science and Technology Organization
Centre for Maritime Research and Experimentation

Viale San Bartolomeo 400, 19126 La Spezia, Italy

[From N. America:
STO CMRE
Unit 31318, Box 19, APO AE 09613-1318]

Tel: +39 0187 527 361
Fax:+39 0187 527 700

E-mail: library@cmre.nato.int